URSI GASS 2021, Rome, Italy, 28 August - 4 September 2021

Effects of thermospheric meridional winds on the interhemispheric asymmetry of the equatorial ionization anomaly over the African sector

A. Loutfi[(1)], F. Pitout[(1)], A.Bounhir[(2)], Z. Benkhaldoun[(2)], and J. J. Makela[(3)]
(1) IRAP, CNES/CNRS/Toulouse University, Toulouse, France.
(2) Oukaimeden Observatory, Laboratory of High Energy Physics and Astrophysics, FSSM, Cadi Ayyad University, Marrakech, Morocco
(3) Department of Electrical and Computer Engineering, University of Illinois at Urbana-Champaign, Urbana, Illinois, USA.

Abstract

Observations made by the Langmuir probe on board the Swarm satellites and Fabry-Perot interferometer (FPI) installed at the Oukaimeden Observatory in Morocco have been systematically analyzed, by making use of three years of measurements from 2014 to 2016, to find the effect of geomagnetic activity on the thermosphere-ionosphere system and the coupling between these two layers. The effect of meridional neutral winds on equatorial ionization anomaly (EIA) crests have been classified during both quiet and disturbed conditions. Over the studied region, the southward meridional winds have the tendency to enhance the northern crest of the EIA during quiet time and in a more pronounced way during geomagnetically disturbed conditions. Moreover, very low electron densities, at times lower than 5×10^3 cm^{-3}, are observed during disturbed conditions. Finally, we have quantified the relations between the FPI data and the EIA, during both quiet and disturbed conditions by introducing an asymmetrical index.

1 Introduction

One of the important phenomena of the equatorial and mid-latitude ionosphere irregularities is the equatorial ionization anomaly (EIA). It is formed as a consequence of the fountain equatorial effect [1], occurring by the upward vertical ExB/B^2 plasma drift that elevates the F-region ionosphere plasma to higher altitudes over the magnetic equator, followed by diffusion along the geomagnetic field lines, that moves the plasma down and away from the equator, forming ionization crests on both sides of the magnetic equator and an ionization trough over the dip equator. The latitudinal plasma distribution that characterizes the EIA (a through at the magnetic equator and two crests at approximately ±17° latitude) is well predicted by many theoretical models [2, 3]. The dynamics of the EIA is significantly influenced by serval parameters. One of them is the thermospheric neutral wind.
Several studies have investigated the interhemispheric asymmetries of the mid-latitude ionosphere, including the asymmetries of the latitudinal positions and intensities of EIA crests. Moreover, the significant longitudinal variations of the EIA interhemispheric asymmetry have been studied in previous works [4, 5], where, the seasonal variability of the interhemispheric asymmetry of the EIA crests with a global view in both solstices and equinoxes have been reported in recent years. One of the prime candidates that govern the EIA variability is the change in magnitude and direction of the neutral wind field initiated by global or local pressure distribution and ambipolar diffusion associated with neutral density and scale height [6]. The EIA asymmetry, not only depend on seasons, solar activity, time, longitudinal and latitude, it also depends on the displacement between the geographic and geomagnetic equators and the magnetic declination angle [5], which is the largest in the American sector. Despite all these studies, the interhemispheric asymmetry of the topside ionosphere needs to be further investigated. Studying the ionosphere-thermosphere coupling has recently become more feasible due to the increasing availability of observations and modelling capabilities. However, many key challenges and issues remain open, as there are large discrepancies in estimates of some of these processes.
This paper aims to present the coupling of the ionosphere-thermosphere during both quiet and disturbed periods through the study of the effect of meridional winds on the EIA crests asymmetry. It is the first time that such a study has been achieved in the Africa sector. Data used in this study were collected during the declining solar cycle (2014-2016). In Section 2, we describe the FPI instrument and methods used to produce the estimates of the thermospheric neutral winds. A brief description of the SWARM instrument is included in this section. Section 3 provides a general classification of the thermospheric-ionospheric response to the storms observed during the studied period. Then, we present an analysis of the disturbed data through the introduced symmetrical index versus the meridional winds. Finally, the last section is devoted to conclusions.

2 Data and method

2.1 Fabry-Perot interferometer

The thermospheric wind data are provided by a Fabry-Pérot interferometer installed at Oukaimeden Observatory in Mo-

rocco (Geographic coordinates: 31.206°N, 7.866°W; magnetic latitude: 22.84°N; elevation: 2700 m) [7]. The FPI [8] measures the thermospheric wind and temperature by observing the 630-nm airglow generated by the dissociative recombination of O^{2+}, which takes place at an average altitude of 250 km approximately. This instrument contains: (1) a sky scanner system having two mirrors with dual-axis that can be moved to point out to any direction (azimuth angle/zenith), (2) a 42-mm diameter etalon with an air gap spacing of 15 mm, (3) a narrow band interference filter to isolate the emission of interest, and finally (4) a thermoelectrically cooled CCD to capture the interference pattern produced by the etalon. The resultant interference pattern is analyzed using the methodology used to analyze the resultant interference pattern described in detail in [9]. We adopt the method detailed in [10] to determine thermospheric wind variability. 545 nights, with FPI data available from 2014 to 2016, were classified according to two geomagnetic indices, SYM-H and Kp. We have 504 quiet nights referring to SYM-H≥-20 and Kp≤2, and 41 disturbed nights with SYM-H≤-50 and Kp≥5. This classification (quiet and disturbed days) will be presented for creating the ionosphere-thermosphere coupling.

2.2 Swarm

Swarm is a European Space Agency mission designed to study the Earth's magnetic field [11]. It's a constellation of three satellites equipped with identical instruments and placed on polar orbits (inclination 87.55°), which accommodate a comprehensive payload designed to measure the magnetic field, but also all the features that can locally modify it. Swarm A and C are located at 460 km of altitude whereas Swarm B is flying at 530 km. Langmuir Probes (LP) in Swarm satellites allow to estimate the electron density (Ne) and temperature (Te) of a plasma. In the next section, we will analyze the variation of the electron density as a function of magnetic latitude and in different local time (LT) sectors. Most of the processes occurring in the ionosphere have a marked magnetic latitudinal dependence [12]. So, we converted geographical coordinates into quasi-dipole coordinates [13]. Swarm Alpha (A), Swarm Bravo (B), and Swarm Charlie (C) satellites are named hereafter SWA, SWB, and SWC, respectively. For creating climatologies of the ionosphere electron density, we have selected all swarm satellite passes that cross a rectangle of -60°S, 60°N in magnetic latitude and -7.88°-4°W and -7.88°+4°W in geographic longitude.

3 The Thermosphere-Ionosphere coupling

The thermospheric neutral wind, especially its meridional component, has a very important effect on the final configuration of the EIA. Figure 1 shows four examples of the electron density response to disturbed (top four panels) and quiet nights (bottom four panels) and the corresponding meridional neutral wind. By analyzing the observed data obtained from Swarm satellites (electron density) with the

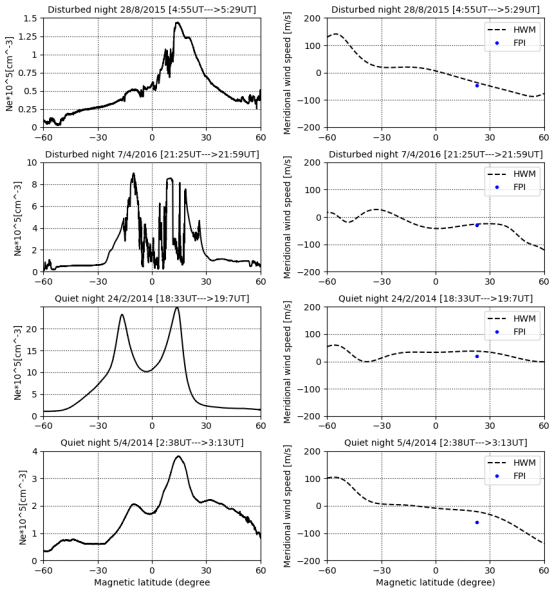

Figure 1. Four examples of response of the electron density to disturbed (four top panels) and quiet nights (four bottom panels). All left panels show the electron density recorded by the Langmuir probe on board a Swarm spacecraft. All right panels show the corresponding meridional wind speed given by the HWM14 model with a dot which represents the closest FPI measurement (positive values are northward meridional winds).

meridional wind speed obtained by Fabry-Perrot interferometer over the studied area, two typical types of EIA crests response are shown in the present section: 1) asymmetrical EIA crests and 2) symmetrical EIA crests with respect to the equator. Both cases are observed during both quiet and disturbed conditions.

From our observations, the case of a symmetrical EIA crests most likely is generated by either weak wind speeds or by converging/diverging winds with about the same velocity in both hemispheres. On the other hand, a northward or southward trans-equatorial meridional wind is a good candidate for this EIA asymmetry generation. More details concerning this analysis will be available in a forthcoming paper where Fabry-Perrot and Swarm data are used along with HWM14 winds simulation results. From observed results most ionospheric electron density provided by Swarm during geomagnetically disturbed conditions are much lower than correspondent quiet time.

The Swarm data have been sorted by seasons (equinoxes and solstices) in order to relate more accurately to the wind data. We introduce an asymmetry index equal to the difference between electron density values at northern $(Ne)_{nc}$ and southern $(Ne)_{sc}$ EIA crests divided by their average (see equation (1)).

$$a = \frac{2 * [(Ne)_{nc} - (Ne)_{sc}]}{(Ne)_{nc} + (Ne)_{sc}} \quad (1)$$

The figure 2 and 3 show meridional wind speed as a function of the index (a) over 3 years. (a) was calculated for

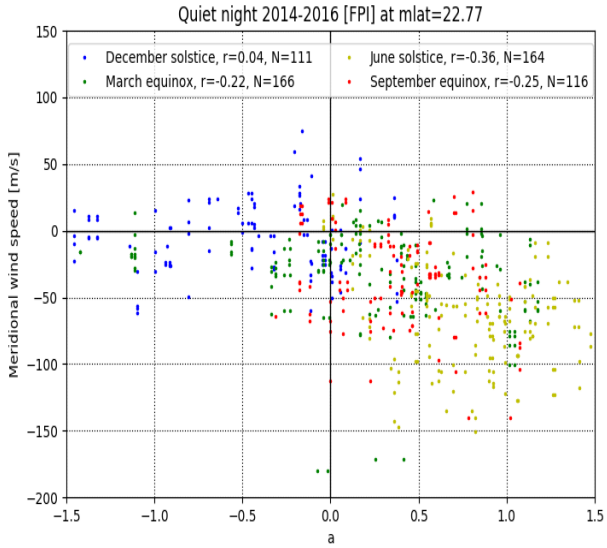

Figure 2. Meridional wind speed as a function of the index (a) over 3 years of all the pass satellites SWA, SWB, SWC during quiet nights of FPI data for all seasons: around December solstice (blue points), March equinox (green points), June solstice (yellow points), and September equinox (red points). Positive values are northward meridional winds.

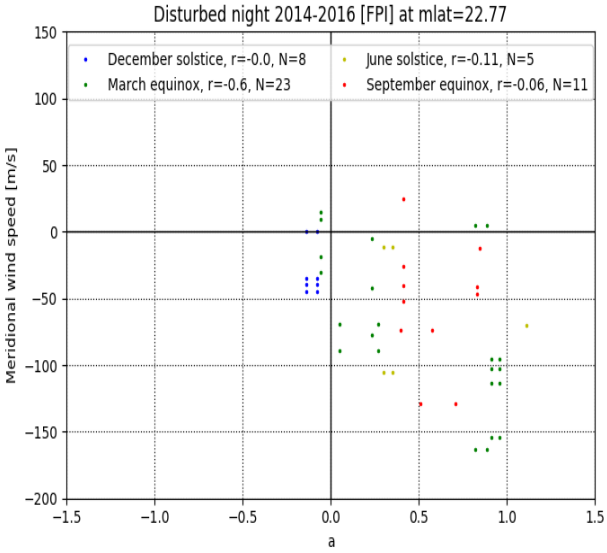

Figure 3. Meridional wind speed as a function of the index (a) over 3 years of all the pass satellites SWA, SWB, SWC during disturbed nights of FPI data for all seasons: around December solstice (blue points), March equinox (green points), June solstice (yellow points), and September equinox (red points). Positive values are northward meridional winds.

each satellite (SWA, SWB, SWC) overflight during quiet and disturbed nights of FPI data. The data are sorted by season: around December solstice (blue points), March equinox (green points), June solstice (yellow points), and September equinox (red points). Positive values are northward for meridional winds.

It is evident that the asymmetry of the EIA crests is the most probable phenomena with the northern crest higher than the southern one (more data points in the bottom right quadrant of 2 and 3). This is first due to the fact that our observations are biased by the single instrument we have in the northern hemisphere only. This behaviour is also related to the direction of the meridional winds that are equatorward during most of the night around March equinox, September equinox and June solstice. However, during the December solstice, meridional winds are northward and their equatorial component is very low. This explains the EIA crests asymmetry with the southward component higher than the northward one. In case of geomagnetic storms, the EIA asymmetry is pronounced in the northern one because of the equatorward component of the disturbed winds due to sudden storm energy deposition. The climatology of the meridional wind [15] during both quiet and disturbed conditions explain the observed EIA crests asymmetries.

4 Conclusions

The effect of geomagnetic activity on the thermosphere-ionosphere system and the coupling between the two layers over 3 years from 2014 to 2016 has been studied using the Langmuir probe on board the Swarm satellites and Fabry-Perot interferometer (FPI) installed at the Oukaimeden Observatory in Morocco. The effects of the meridional wind on the interhemispheric asymmetry of the EIA on the African sector during both quiet and disturbed nights, leading to the following main conclusions:

1. Two typical types of EIA crests response are shown. The first type have characterised by the asymmetrical EIA crests, however the second type is presented by symmetrical EIA crests with respect to the equator. Both cases are observed in both quiet and disturbed conditions.

2. The relations between the FPI data, the EIA crests, and HWM model outbut, during both quiet and disturbed conditions have been quantified. A stronger equatorward wind fields a strong EIA asymmetry with a denser ionisation crest in the northern hemisphere. However, the degree of such asymmetry depends upon the competing forces of the wind velocity and the seasons.

This preliminary study is obviously limited by our instrumental setup: an FPI in the southern hemisphere and in the same local time sector would advantageously complement our study. Unfortunately, such an instrument does not yet

exist. A way of having further information about thermospheric winds in the southern hemisphere would be to use a numerical model such as HWM. This will be the next stage of our study.

5 Acknowledgements

This project is financially supported by Campus France through the French-Moroccan bilateral program "PHC Toubkal 2019" (grant number: 41409WJ). The LOS wind data used in this study is freely available for use in the Madrigal database http://madrigal.haystack.mit.edu/madrigal/. Swarm data were retrived from ESA's Earth Online website: https://earth.esa.int/web/guest/swarm/data-access. The SYM-H index storm can be downloaded from (https://omniweb.gsfc.nasa.gov/). The International Service of Geomagnetic Indices (ISGI) is in charge of the elaboration and dissemination of geomagnetic indices(Kp).

References

[1] Appleton, E. V. (1946). Two anomalies in the ionosphere. *Nature*,157(3995), **691**. doi: https://doi.org/10.1038/157691a0.

[2] Hanson, W. B., and Moffett, R. J. (1966). Ionization transport effects in the equatorial fregion. *Journal of Geophysical Research*, **71(23), 55595572**. doi: https://doi.org/10.1029/JZ071i023p05559

[3] Bittencourt, J. A., Pillat, V. G., Fagundes, P. R., Sahai, Y., and Pimenta, A. A. (2007). Lion: A dynamic computer model for the low-latitude ionosphere. *Annales Geophysicae*, **25(11), 23712392**. doi: https://doi.org/10.5194/angeo-25-2371-2007

[4] Lin, C. H., Liu, J. Y., Fang, T. W., Chang, P. Y., Tsai, H. F., Chen, C. H., and Hsiao, C. C. (2007). Motions of the equatorial ionization anomaly crestsimaged by formosat-3/cosmic. *Geophys. Res. Lett.*,**34, L19101**, https://doi.org/10.1029/2007GL030741

[5] Luan, X., Wang, P., Dou, X., and Liu, Y. C.-M. (2015). Interhemispheric asymmetry of the equatorial ionization anomaly in solstices observed by cosmic during 20072012. *J. Geophys. Res. Space Physics*, **120 , 30593073**, https://doi.org/10.1002/2014JA020820

[6] Kelley, M. (2009). The earths ionosphere. International Geophysics (Book 96) 2nd edn. Academic Press, San Diego.

[7] Makela, J. J., Meriwether, J. W., Lima, J. P., Miller, E. S.,and Armstrong, S. J. (2009). The remote equatorial nighttime observatory of ionospheric regions project and the international heliospherical year. *Earth Moon Planet* **457 104:211226**. doi:10.1007/s11038-008-9289-0

[8] Makela, J. J., Meriwether, J. W., Huang, Y., and Sherwood, P. J. (2011). Simulation and analysis of a multi-order imaging fabryperot interferometer for the study of thermospheric winds and temperatures. *Appl. Optics*, **50, 44034416**, https://doi.org/10.1364/AO.50.004403

[9] Harding, B. J., Gehrels, T. W., and Makela, J. J. (2014). Nonlinear regression method for estimating neutral wind and temperature from fabryperot interferometer data. *Appl. Optics*, **53, 666- 673**. doi: 10.1364/AO.53.000666

[10] Fisher, D. J., Makela, J. J., Meriwether, J. W., Buriti, R. A., Benkhaldoun, Z., Kaab, M., and Lagheryeb, A. (2015). Climatologies of nighttime thermospheric winds and temperatures from fabry-perot interferometer measurements: From solar minimum to solar maximum. *J. Geophys. Res.-Space*, **120, 66796693**, doi: 10.1002/2015JA021170

[11] Friis-Christensen, E., Lhr, H., Knudsen, D., and Haagmans, R. (2008). Swarm an earth observation mission investigating geospace. *Advances in Space Research*, **41(1), 210216**. doi: doi:10.1016/j.asr.2006.10.008

[12] Davies, K. (1990). Ionospheric radio. Peter Peregrinus Ltd., London. Drob, D. P., Emmert, J. T., Meriwether, J. W., Makela, J. J., Doornbos, E., Conde, M., . . . Klenzing, J. H. (2015). An update to the horizontal wind model hwm: The quiet time thermosphere. *Earth Space Sci.*, **2, 301319**. doi:10.1002/2014EA000089

[13] Emmert, J., Richmond, A., and Drob, D. (2010). A computationally compact representation of magnetic-apex and quasi-dipole coordinates with smooth base vectors. *J Geophys Res*. doi: 10.1029/2010JA015326.

[14] Link, R., and Cogger, L. (1988). A reexamination of the oi 6300- nightglow. *J. Geophys. Res.-Space*, **93, 98839892**, doi: doi:10.1029/JA093iA09p09883.

[15] Loutfi, A., Bounhir, A., Pitout, F., Benkhaldoun, Z., and Makela, J. J. (2020). Thermospheric neutral winds above the oukaimeden observatory: Effects of geomagnetic activity. *Journal of Geophysical Research: Space Physics*, **125, e2019JA027383**, https://doi.org/10.1029/2019JA027383